3-Phase Rectifier System with very demanding dynamic load: Architecture Analysis and Control Strategy

J. M. Molina, S. Zhao, J. Oliver, P. Alou, O. García, J.A. Cobos
Centro de Electrónica Industrial
Universidad Politécnica de Madrid
Madrid, Spain

***Abstract*—A distributed power architecture for aerospace application with very restrictive specifications is analyzed. Parameters as volume, weight and losses are analyzed for the considered power architectures. In order to protect the 3 phase generator against high load steps, an intermediate bus (based in a high capacitance) to provide energy to the loads during the high load steps is included.**
Prototypes of the selected architecture for the rectifier and EMI filter are built and the energy control is validated.

***Index Terms*—Power Distribution System, EMI, Energy Control.**

I. INTRODUCTION

THE aerospace applications have recurrent requirements in parameters as volume, weight or efficiency. These requirements are constrained by the specifications of the system such as the standards MIL-STD-704F, MIL-STD-461E, military derating in the components selection, and galvanic isolation.
The MIL-STD-461E is very restrictive in comparison with others standards for the EMI filter design in terms of frequency range. This standard is applicable from 10 kHz. This frequency is relatively low compared with the typical switching frequency of the actual rectifiers for applications under 10 kW [1]-[4], increasing the weight and volume of the EMI filter.
In aerospace applications, the optimization of the whole distributed power system, from the electrical generator to the loads, is a common practice [5], analyzing different architectures to optimize the system in terms of weight, volume, losses and reliability.
The system analyzed in this paper has an intermediate bus, based on a high capacitance. The intermediate bus is included to protect the generator during high load steps. A control strategy is proposed in order to control this bus.

In section II the optimum architecture for an AC/DC system formed by independent loads supplied from a 115 V 400 Hz generator with a total power of 13kW is analyzed.

In section III a Control Strategy to protect the generator against high load steps is proposed.

In section IV the validation of the control and the experimental results are shown.

II. POWER SYSTEM ARCHITECTURE

The Power Architecture analysis is presented in this section.

A. System Specifications

The system analyzed in this work has to comply with the followings specifications:

- Input Voltage: 115V RMS phase to neutral point
- Main frequency: 400Hz
- Nominal Bus Voltage(V_o): 200 V
- Range of Bus Voltage (V_o): 180V to 250 V
- Rated output power: 13 kW
- Comply with MIL-STD-704F
- Comply with MIL-STD-461E
- Military derating
- Galvanic isolation
- Ambient temperature: 70 ºC
- Switching Frequency externally synchronized

The Military derating that has been considered is: 70 % in diodes voltage, 75 % in transistor current, 70 % in transistor voltages and 110 ºC as maximum temperature in magnetic cores.
To achieve galvanic isolation the system is divided in two stages, a rectifier stage and a DC/DC stage with isolation.
The system is equipped of an intermediate bus between the rectifier and the DC/DC. This bus provides the energy demanded by the load during high load steps. The basic structure of the system is shown in Fig. 1.

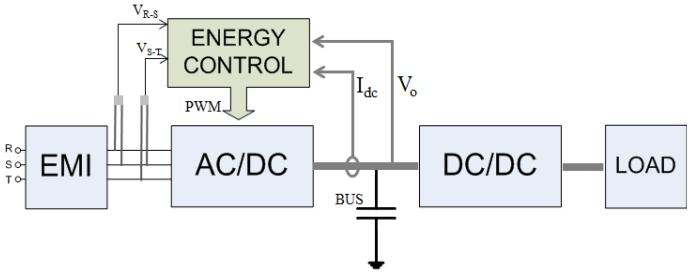

Fig. 1. Block diagram of the system

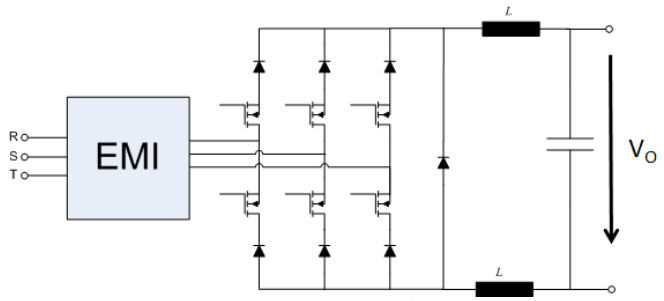

Fig. 2. Three phase buck type rectifier with EMI filter

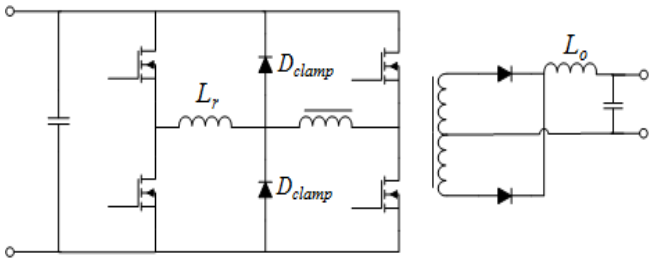

Fig. 3. Full Bridge Phase Shift with clamping diodes and additional inductance (Lr).

B. *Topology Selection*

The system is formed by the EMI filter, two power stage and one intermediate bus (Fig. 1). The topologies selected are explained and justified in this subsection.

1) Rectifier

One of the principal requirements of this system is to manage the intermediate bus. Consequently, the rectifier topology has to be controlled.

To obtain a high power density and high efficiency, the three phase buck-type rectifier (Fig. 2) has been selected. This unidirectional topology is commonly proposed for aerospace and aircraft applications [6]. This topology does not need a start-up circuit and can maintain the sinusoidal input current shape after one main phase failure.

In [7] and [8] several modulations methods for this rectifier have been analyzed. The principal differences between the modulations methods are the switching losses and the ripple in the DC inductor. The modulation based on Method 1 is the best in terms of losses for this application. In Section D, the optimum switching frequency is analyzed.

The control of the rectifier is analyzed in detail in Section III.

2) DC/DC:

For this application a Full-Bridge Phase Shift (FBPS) has been selected. FBPS is a very popular topology in the range of a few kilowatts [9]. The specifications of galvanic isolation and high power density are satisfied with this topology. Other issues as zero voltage switching can reduce the noise during the commutations in the switches and therefore the noise in the system. In order to improve the efficiency, some elements as an external inductance, to achieve ZVS along the whole range of load, and clamping diodes to protect the circuit again overvoltage oscillation are added to the circuit [10].

The system analyzed in this paper is based on seven FBPS of 2 kW.

C. *EMI*

The EMI filter represents around 30% of the weight of the system [11]. The current spectrum has been analyzed in order to determine the attenuation needed to comply with MIL-STD-461E. The loads are totally independent, consequently it is not possible to apply interleaving among the loads. Therefore, the EMI has to be analyzed for the worst case when all the loads are demanding the maximum power at the same time.

In section D the optimum architecture for the EMI filter is analyzed in terms of weight and losses.

D. *Architecture Analysis*

The optimization analysis determines the best architecture for the system among several options. The principal factors taken into account are the weight, volume and losses.

The goal is to optimize the EMI filter and the rectifier, because the DC/DC is fixed in this work as it is explained in Section B.2). The first step is to determine the nominal switching frequency of the rectifier which is conditioned by the synchronized signals of the loads. This is a specification from Section II.A. Table I shows the frequency ranges analyzed depending on the load.

Table I. Frequency ranges

FREQUENCY RANGES		
Min.	Nominal	Max.
80 kHz	105 kHz	130 kHz
160 kHz	210 kHz	260 kHz

The optimization process is the following:

1) Determine the frequency range and the optimum architecture for the rectifier in terms of weight, volume and losses. Taking into account the worst case for power and frequency in each case.
2) Analyze the current spectrum and the architectures for the EMI filter.

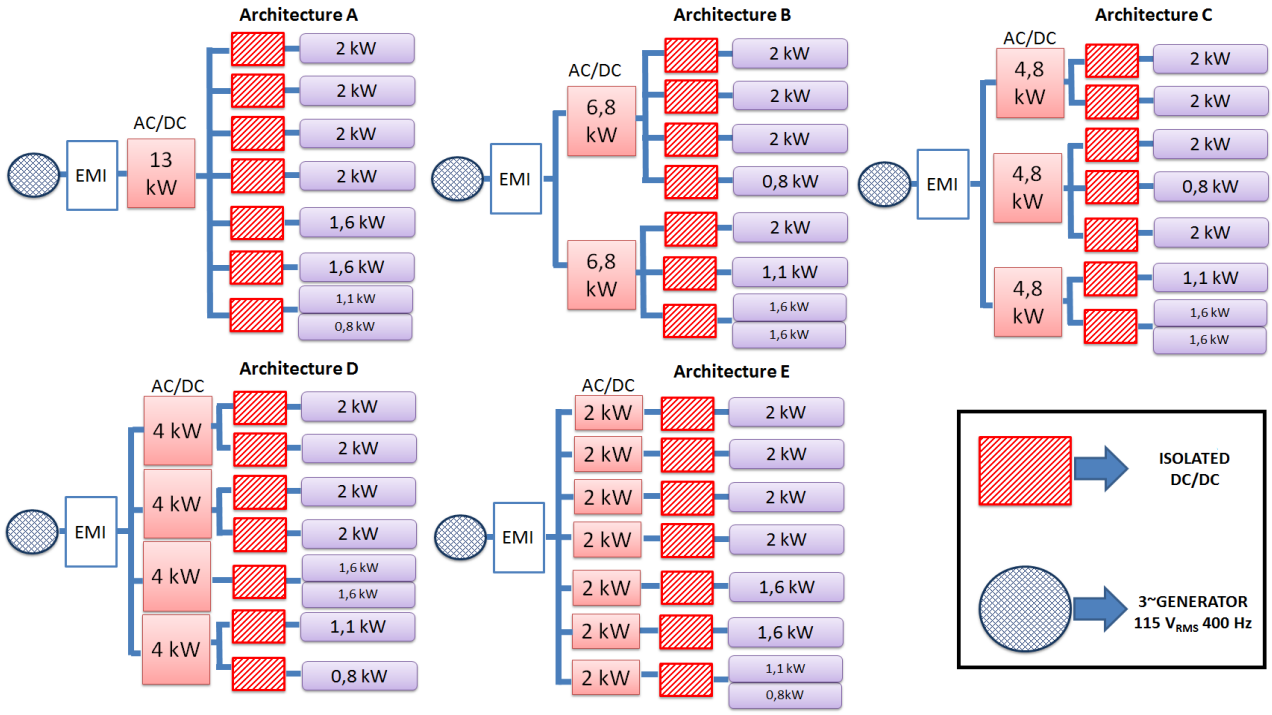

Fig. 4. Architectures proposed

For this application, in order to obtain the optimum architecture solution, the trade-off among several parameters is performed emphasizing the weight and the volume.

1) Power architecture

Seven distributed loads have to be supplied. Fig. 4 shows the architectures analyzed for the power architecture. The estimation of the efficiency and weight/volume of the inductors is presented to select the best architecture. The calculations are presented for the worst case in each architecture, maximum frequency for the semiconductor losses and minimum frequency to design the inductors.

To decide the switching frequency is the first priority. Fig. 5 shows the results in terms of the efficiency, weight and volume.

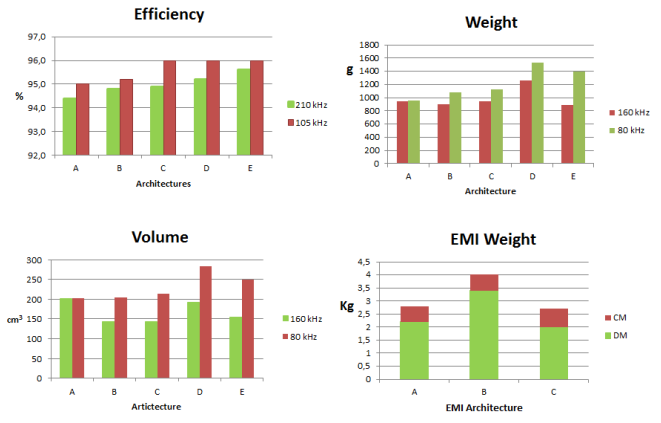

Fig. 5. Estimation of the efficiency of the rectifier and the weight and volume of the inductors for the different architectures. Weight for the EMI architectures

The solutions for the higher frequencies are lighter and smaller, and the differences in the efficiency for the best case (Architecture E) are less than 0,4%, therefore, 210 kHz is selected as switching frequency. Once the frequency is selected, the architectures are analyzed. The weight of the architectures determines that E is the lighter one, with small differences respect to A, B and C. In terms of efficiency C, D and E are similar. In terms of volume, B, C and E are the smallest. Emphasizing in the weight, architecture E is selected. This Architecture is formed by 7 stages of 2 kW. This modularity is considered as an advantage.

2) EMI architecture

Once the frequency range is decided, the current spectrum in the worst case is simulated (13 kW and 160 kHz).

Analyzing the current spectrum of Fig. 7 the attenuation required at 160 kHz to comply with the standard is 100 dBuV. In order to obtain a high cut off frequency in comparison with the generator frequency (400 Hz), only solutions of 2 and 3 stages for the input filter have been analyzed (for the differential mode filter) because the solution of 1 stage has a very low cut off frequency. Both solutions have been analyzed in terms of weight and for these requirements, the solution of 2 stages is the heaviest, hence this solution is rejected. The solution of three stages is adopted with a f_c=21 kHz.

Three different architectures for the EMI filter are proposed in Fig. 6. The Architecture *Concentrate* has 3 stages of differential mode and one of common mode. The Architecture *Partially Distributed* has one differential mode stage for the whole system, and the others two differential mode stages and one common mode stage are distributed in each power channel. The Architecture *Distributed* has in each power channel (7 power channel) three differential mode stages and one common mode stage.

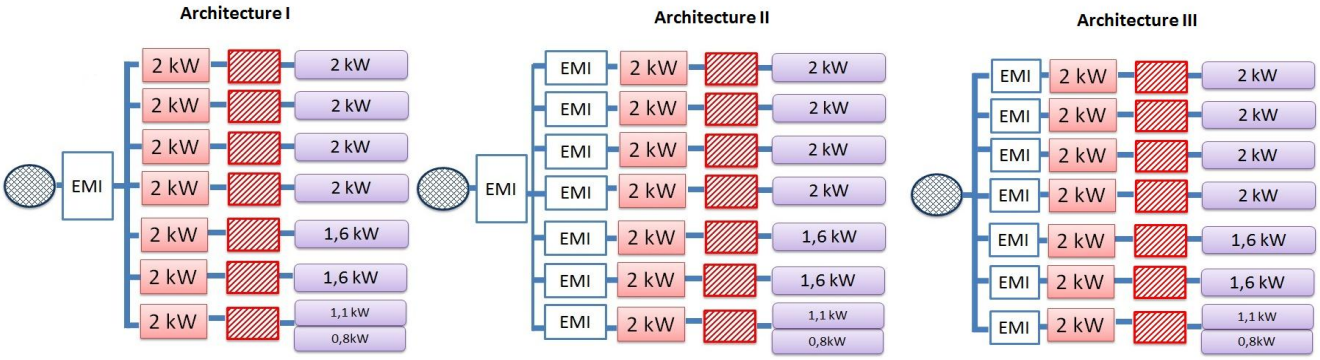

Fig. 6. EMI ARCHITECTURES. I) Concentrated II) Partially distributed III) Distributed

Fig. 5 shows the results of the estimations for the weight in the EMI filter. The architecture selected is the distributed filter because it is the lighter. The modularity of this solution increases the reliability.

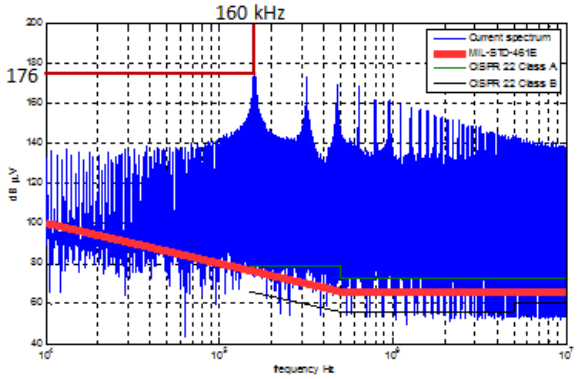

Fig. 7. Current Spectrum at 13kW and switching frequency of 160 kHz

III. CONTROL STRATEGY

A. *Motivation*

This research topic aims at bringing forward a control method against the very demanding dynamic load variation, shown in Fig. 8. P_{load} implies the power load of the whole rectifier system. The control target is to smooth the input current from the three-phase generator while at the same time keeping the bus voltage of the rectifier (V_o) within the proper range. Generally by the normal control approach, the bandwidth of the control loop is configured as high as possible to ensure fast dynamic response. In this way, the power from the input source can be transferred directly to the output avoiding any energy storage in the middle.

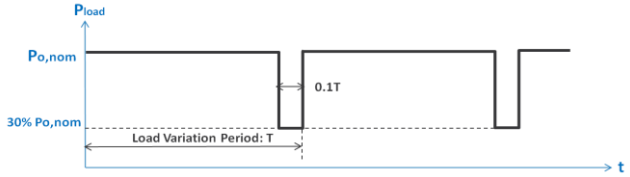

Fig. 8. Characteristic of the Load Steps

If this normal approach is adopted, then the overall system schematic is as Fig. 9. Here, the three-phase buck-type rectifier represents the whole AC/DC stage, Co represents the intermediate bus, and the set of DC/DC converters and loads are substituted by a power source P_{load}. In this case, since the control loop reacts so fast that the injected power through the rectifier will act in the same shape as load power variation. However the shape of input voltage from the three-phase generator always keeps constant, thus the input RMS phase current will behave in the same pulse-like waveform, which is harmful to the generator for the sake of reliability.

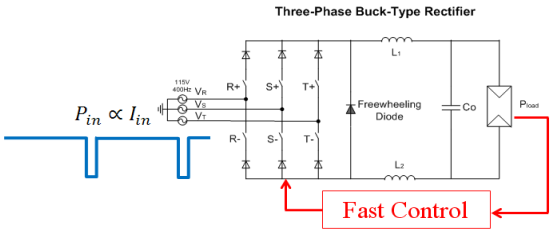

Fig. 9. Typical control approach

On the contrary, a slow control loop is preferred for this application. Seen in Fig. 10, a smoothly varied power is injected through the rectifier against the pulse-wave load power. As a consequence, the energy difference between the input power and the power demanded by the load is handled by the output capacitor C_o, being necessary a higher capacitance to keep bus voltage under regulation.

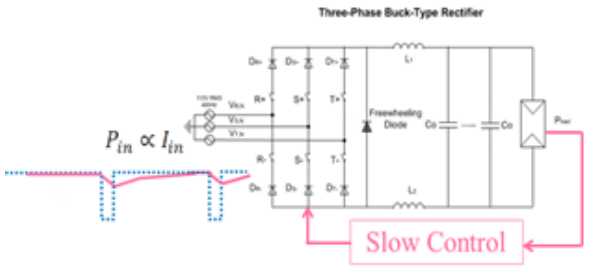

Fig. 10. Energy Control proposed

B. *Control Method*

Fig. 11 shows the averaged plant model for the rectifier system being considered. The buck-type rectifier is modeled as current source with values $I_{g,}$ while the DC/DC with its load is represented as power source P_{load}.

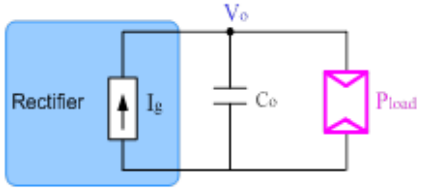

Fig. 11. Plant model of buck rectifier

The time-domain equation for the plant model can be described as

$$C_O \frac{dv_O(t)}{dt} = i_g(t) - \frac{p_{load}(t)}{v_O(t)} \quad (1)$$

The transfer function of v_o over i_g is

$$\frac{\hat{v_o}(s)}{\hat{i_g}(s)} = \frac{-R_{eq}}{1 - R_{eq}C_o \cdot s} \quad (2)$$

where R_{eq} denotes the load equivalent resistance at operating point,

$$R_{eq} = \frac{V_{o,nom}^2}{P_{o,nom}^2} = \frac{200V^2}{13000W} = 3.077\Omega \quad (3)$$

Notably, the term $-R_{eq}C_o$ in the denominator of Eq. (2) introduces a Right Half Plane Pole. In order to ensure stability, it is necessary to implement a big loop gain to encircle (-1, j0) point anticlockwise in Nyquist plot. However, this is contradictory to the preferred control strategy of slow bandwidth.

Thus, another transfer function is derived with a term $v_o(t)$ multiplied to both sides of (1);

$$v_O(t)C_O \frac{dv_O(t)}{dt} = v_O(t)i_g(t) - p_{load}(t) \quad (4)$$

Notably, $v_o(t)C_o dv_o(t)/dt$ happens to be the derivative of energy in the output capacitance over time. Thus, there stands

$$\frac{d\varepsilon_c(t)}{dt} = p_g(t) - p_{load}(t) \quad (5)$$

It is straight forward to obtain the transfer function of $\varepsilon_c(s)$ over $p_g(s)$ like

$$\frac{\hat{\varepsilon_c}(s)}{\hat{p_g}(s)} = \frac{1}{s} \quad (6)$$

If the rectifier is controlled as a power source during the load transients and, instead of controlling the bus voltage (V_o), the energy stored in C_o is controlled, based on the plant model of Eq. (6), thus, there is no restriction in the decision of the system bandwidth, being a trade-off between the energy stored in C_o and the load transient demanded to the three phase generator. As a result, in the following control alternatives, the energy in the output capacitance is monitored and used to control the power injected through the rectifier. This idea comes from passivity based control [13]. Here, two different type of controllers based on the issue of slow energy control loop are discussed.

1) PI Controller

Based on the plant model derived in Eq. (6), a PI controller is designed and implemented as the block diagram in Fig. 12, where the rectifier is controlled as a power source P_g.

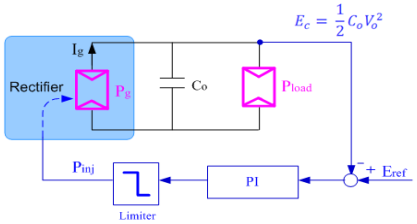

Fig. 12. Block diagram for the PI controller

In all the following designs, the same capacitance value Co=34mF is adopted as a standard. The transient response of the averaged model with the smallest bandwidth of 0.8Hz is depicted in Fig. 13.

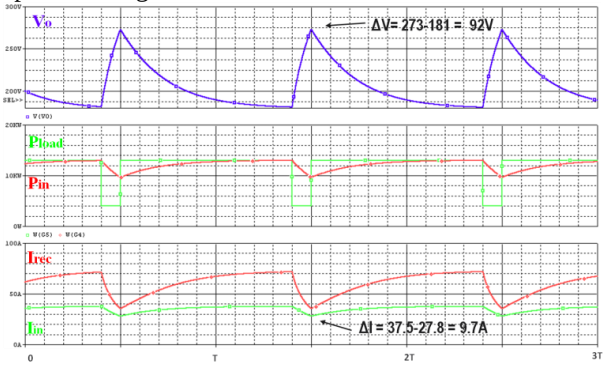

Fig. 13. Transient response of PI controller with a bandwidth of 0.8Hz

It is obvious that once the capacitance choice is made based on the allowed volume and weight in the prototype, with the augment of the bandwidth, the power injected through the rectifier reacts faster and closer to the shape of load power variation. Consequently the energy handled by the capacitor decreases, which leads to the decrease on output voltage variation, meanwhile since the power is injected faster, the phase input RMS current (I_{in} in Fig. 13) responds faster at the same time.

On the other hand, by keeping at the same bandwidth, the injected power of the rectifier behaves exactly the same. Thus, bigger capacitance indicates more capacitance available for handling the same amount of energy difference when load step occurs. Accordingly, the variation of v_o decreases, while the variation of input phase current does not show any changes.

2) Proportional Controller and Feed-Forward of the Load Power (P+FF)

The other control alternative is also proposed with a feed-forward path included into the energy controller, and the block diagram is shown as Fig. 14.

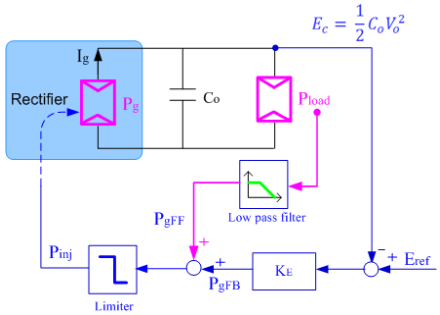

Fig. 14. Block diagram for P+FF controller

Eq. (3) is still valid under this condition. Furthermore, feed-forward of the load power through a low pass filter is added to the feed-back path and eventually the sum provides the power that should be injected through the rectifier. Thus, at the summing node, there exists

$$p_g = p_{gFF} + p_{gFB} \quad (7)$$

and also

$$p_{gFF} = LPF(p_{load}(t)) \quad (8)$$

Substitute P_g in (5) with the one in (7), eventually

$$\frac{d\hat{\varepsilon_c}(t)}{dt} = \hat{p}_{gFB}(t) \quad (9)$$

Up to now, a plant model of only an integrator is derived without output power disturbance, and the transfer function is

$$\frac{\hat{\varepsilon_c}(s)}{\hat{p_{gFB}}(s)} = \frac{1}{s} \quad (10)$$

For this plant model, it is not required an integral action since most of the reference for injected power comes from the feed-forward path. As a result, only a proportional controller is capable enough to maintain stability and handle the transients. Thus with the smallest bandwidth of 0.16Hz in this case, the transient response of the average model is shown in Fig. 15.

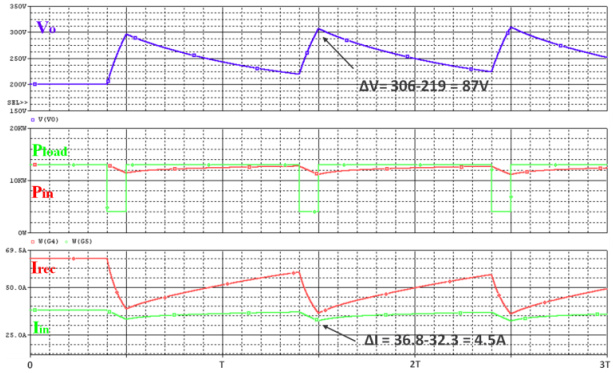

Fig. 15. Transient response of P+Feedforward controller at bandwidth of 0.16Hz

3) Comparison between PI controller and P+FF controller

PI and P+Feed-forward controller are compared in Table II. Inside this table, it can be concluded that both of the control methods are good, since at a certain bandwidth, the transient behavior of PI control and P+FF control are similar, however P+FF control is preferable since a lower bandwidth for the system can be reached.

Table II. Comparison between PI and P+FF controller

	BW=0.8Hz	BW=1.6Hz	BW=4Hz	BW=8Hz
PI Controller	$\Delta V_O = 92V$ $\Delta I_{iin} = 9.7A$	$\Delta V_O = 74V$ $\Delta I_{iin} = 15.4A$	$\Delta V_O = 47V$ $\Delta I_{iin} = 23A$	$\Delta V_O = 29V$ $\Delta I_{iin} = 24.9A$
	BW=0.16Hz	BW=1.6Hz	BW=4Hz	BW=8Hz
P+FF Controller	$\Delta V_O = 87V$ $\Delta I_{iin} = 4.5A$	$\Delta V_O = 71V$ $\Delta I_{iin} = 16.7A$	$\Delta V_O = 47V$ $\Delta I_{iin} = 23.5A$	$\Delta V_O = 30V$ $\Delta I_{iin} = 25.1A$

IV. SYSTEM VALIDATION

The control is validated by simulation and experimentally in a prototype.

1) Proposed Control Simulation

The Energy Control applied to a switching model of the rectifier, including the EMI filter is validated in this section.
Two control loops are implemented in the circuit at the same time, the faster one with bandwidth of 4Hz while the slow one with bandwidth of 1,6Hz.
Inside the nominal output voltage range only the slower control is introduced into the loop; while V_o goes out of this range, the faster control is making effect and the slower one is disconnected, therefore, the faster control can prevent V_o from going out of the nominal range. The switching model of the rectifier together with the energy control loop is built in PSIM, and the transient response is shown in Fig. 16.

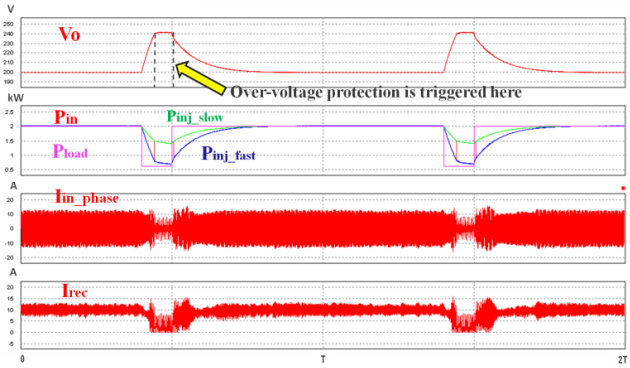

Fig. 16. Transient response for switching model simulation of the system applying P+FF control and over-voltage under-voltage techniques

2) Prototype Validation

A 2 kW 3 phase buck type rectifier and an EMI filter has been built in order to validate the energy control and verify that the architecture selected comply with the system specifications. Fig. 17 shows waveforms of the inductor current and input current of one phase for the system working at 2 kW (Input voltage: 115 V_{rms}, Vo=206 V) with an efficiency of 96% and THD= 5%.

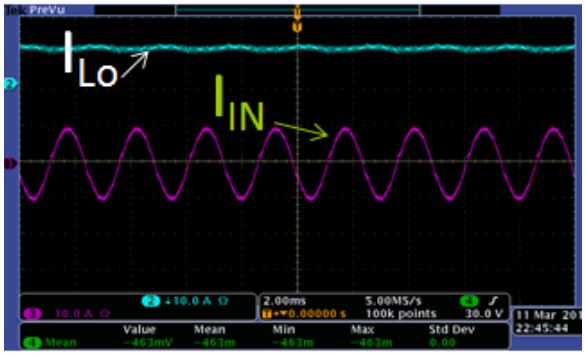

Fig. 17. Inductor current and input current for one phase.

V. CONCLUSION

The power architecture and the energy control strategy for a 13kW system have been analyzed and presented in this paper.

Three critical specifications make this system very different from typical applications:

1) The switching frequency must be synchronized with an external reference which can range between 80 kHz-130 kHz and multiples.

2) The loads have a demanding transient behavior, changing from 4 kW to 13 kW.

3) To increase the reliability of the three phase generator, it is proposed to protect the generator from the load steps by increasing the output capacitance of the rectifier and slow down the bandwidth of the control.

Five power distribution architectures and 3 architectures for the EMI filter have been analyzed. The architecture selected is a distributed architecture based on rectifiers of 2 kW and EMI filters for each rectifier.

The main advantage of this solution is the modularity, besides the fully distributed solution is among the solutions with best efficiency and less weight.

The output voltage of the rectifier cannot be controlled with a classical control since it is loaded with a power source, creating a right half plane pole in the system and making mandatory a high bandwidth to stabilize the system. The paper proposes to control the rectifier as a power source and controlling the energy of the output capacitance instead of the output voltage.

Applying this control, the RHP pole is eliminated, becoming the bandwidth a free design variable and making possible the use of a slow bandwidth in the system.

A prototype of a 2kW rectifier cell is built together with the inner loop for modulation of the six switches. Experimental results for P_o=2 kW are shown.

REFERENCES

[1] J. S. Cloyd, “Status of the united states air force’s more electric aircraft initiative,” IEEE Aerospace and Electronic Systems Magazine, vol. 13, no. 4, pp. 17–22, 1998.

[2] W. G. Homeyer, E. E. Bowles, S. P. Lupan, P. S. Walia, and M. A. Maldonado, “Advanced power converters for more electric aircraft applications,” in Proc. 32nd Intersociety Energy Conversion Engineering

[3] D. Izquierdo, R. Azcona, F. del Cerro, C. Fernandez, and B. Delicado,“Electrical power distribution system (hv270dc), for application in more electric aircraft,” in Proc. Twenty-Fifth Annual IEEE Applied Power Electronics Conf. and Exposition (APEC), 2010, pp. 1300–1305.

[4] R. I. Jones, “The more electric aircraft: the past and the future?” in Proc. IEE Colloquium Electrical Machines and Systems for the More Electric Aircraft (Ref. No. 1999/180), 1999..

[5] Lee, F.C.; Ming Xu; Shuo Wang; Bing Lu; , "Design Challenges For Distributed Power Systems," Power Electronics and Motion Control Conference, 2006. IPEMC 2006. CES/IEEE 5th International , vol.1, no., pp.1-15, 14-16 Aug. 2006.

[6] M. Silva, N. Hensgens, J. Oliver, P. Alou, O. Garcia, and J. Cobos, “New considerations in the input filter design of a three-phase buck-type pwm rectifier for aircraft applications,” in Energy Conversion Congress and

[7] M. Baumann, T. Nussbaumer, and J. W. Kolar, “Comparative evaluation of modulation methods of a three-phase buck + boost pwm rectifier.part i: Theoretical analysis,” IET Power Electronics, no. 2, pp. 255–267,

[8] T. Nussbaumer, M. Baumann, and J. W. Kolar, “Comparative evaluation of modulation methods of a three-phase buck + boost pwm rectifier. part ii: Experimental verification,” IET Power Electronics, no. 2, pp. 268–274, 2008.

[9] J.A. Sabate,V. Vlatkovic, R.B. Ridley, F.C. Lee, B.H. Cho, "Design considerations for high-voltage high-power full-bridge zero-voltage-switched PWM converter," Applied Power Electronics Conference and Exposition, 1990. APEC '90, Conference Proceedings 1990., Fifth Annual , vol., no., pp.275-284, 11-16 March 1990.

[10] R. Redl, N.O. Sokal, L. Balogh, "A novel soft-switching full-bridge DC/DC converter: Analysis, design considerations, and experimental results at 1.5 kW, 100 kHz," Power Electronics Specialists Conference, 1990. PESC '90 Record., 21st Annual IEEE , vol., no., pp.162-172, 0-0 1990.

[11] M. Heldwein and J. Kolar, “Impact of emc filters on the power density of modern three-phase pwm converters,” Power Electronics, IEEE Transactions on, vol. 24, no. 6, pp. 1577 –1588, june 2009.M. Young, *The Techincal Writers Handbook.* Mill Valley, CA: University Science, 1989.

[12] R.D. Middelbrook, “Input filter considerations in design and application of switching regulators”IEEE 1976.

[13] Alarcon. G, Cardenas. V, Ramirez. S, Visairo. N, Nunez.C, Oliver. M, Sira Ramirez H., "Nonlinear passive control with inductor current feedback for an UPS inverter," Power Electronics Specialists Conference, 2000. PESC 00. 2000 IEEE 31st Annual , vol.3, no., pp.1414-1418 vol.3, 2000